Proceedings of the 7th International Young Geotechnical Engineers Conference – Scott (Ed.)

Pseudo-static stability analysis of caisson in porous media

Analyse de Stabilité Pseudo-Statique de Caisson en Milieu Poreux

Mohit Kumar & Kaustav Chatterjee
Department of Civil Engineering, Indian Institute of Technology Roorkee, Roorkee, India, mkumar2@ce.iitr.ac.in

ABSTRACT: Caissons are rigid foundation systems which are used to support lifeline structures like bridges. In the current study, 3D model of a square caisson embedded in saturated sand overlying clay bed has been modeled in finite element analysis based computer program ABAQUS. Mohr-Coulomb plasticity model has been used for modeling of sand whereas modified cam clay model has been used for clay. Horizontal seismic acceleration coefficient (k_h) is varied as 0.1, 0.2 and 0.3. For each value of k_h, the value of vertical seismic acceleration coefficient (k_v) is varied as $0k_h$, $0.5k_h$ and $1.0k_h$. Static loading conditions have also been modeled for comparison of results. In addition to the body force, vertical and lateral loads are also applied on the caisson and its effect is measured in terms of soil resistances applied on caisson. The mesh and boundary conditions of the model is validated using results of experimental study by Sharda (1975). It is observed that with increase in values of k_h and k_v, the stability of caisson reduces which is evident from the reduced value of moment at scour level and smaller value of depth of point of rotation.

RÉSUMÉ : Les caissons sont des systèmes de fondation rigides qui sont utilisés pour soutenir les structures de ligne de vie comme les ponts. Dans la présente étude, le modèle 3D d'un caisson carré noyé dans du sable saturé recouvrant un lit d'argile a été modélisé dans le programme informatique ABAQUS basé sur l'analyse par éléments finis. Le modèle de plasticité de Mohr-Coulomb a été utilisé pour la modélisation du sable tandis que le modèle modifié d'argile à cames a été utilisé pour l'argile. Le coefficient d'accélération sismique horizontale (k_h) varie de 0.1, 0.2 et 0.3. Pour chaque valeur de k_h, la valeur du coefficient d'accélération sismique verticale (k_v) varie en 0kh, $0.5k_h$ et $1.0k_h$. Les conditions de chargement statique ont également été modélisées pour la comparaison des résultats. En plus de la force du corps, des charges verticales et latérales sont également appliquées sur le caisson et son effet est mesuré en termes de résistances du sol appliquées sur le caisson. Le maillage et les conditions aux limites du modèle sont validés à l'aide des résultats de l'étude expérimentale de Sharda (1975). On observe qu'avec l'augmentation des valeurs de k_h et k_v, la stabilité du caisson diminue, ce qui est évident à partir de la valeur réduite du moment au niveau de l'affouillement et de la valeur plus petite de la profondeur du point de rotation.

KEYWORDS: Caisson; pseudo-static; ABAQUS; porous media; modified cam clay model

1 INTRODUCTION

Caissons are massive foundation system with high rigidity enabling it to withstand large magnitudes of vertical load, lateral load and moment. This makes caissons well suited as foundation system for structures subjected to such loads.

Under the action of the imposed loads, soil resistances in the form of lateral soil pressure, horizontal and vertical skin friction, base pressure and base friction as shown in Figure 1.

1.1 *Review of literature*

The studies pertaining to caissons have been going on for eight decades. Several researchers have carried out theoretical, experimental and numerical studies in this duration. Theoretical analysis has been the oldest approach for studying caisson behavior (Terzaghi, 1943; Pender, 1947; Banerjee and Gangopadhyay, 1960; Dominguez, 1978; Gerolymos and Gazetas, 2006; Biswas and Chowdhury, 2019; Biswas and Chowdhury, 2020).

Experimental studies have also been carried out by several researchers wherein researchers carried out a series of laboratory tests, field tests and centrifuge tests on caisson models (Sharda, 1975; Gadre and Dobry, 1998; Olson et al., 2017).

Numerical study has been adopted in the past three decades in order to simulate different soil profiles, loading conditions, soil and interface properties, input motion etc (Mitta and Luco, 1989; Varun et al., 2009; Gerolymos et al., 2015; Kumar and Chatterjee, 2020; Kumar and Chatterjee, 2021). Finite element method and finite difference method are the most common approaches for numerical study. Software packages like ABAQUS, PLAXIS and FLAC are usually adopted to carry out the highly computational numerical analysis.

In the present study, square caisson embedded in layered soil has been modeled using finite element method based software ABAQUS. Based on the pseudo-static numerical analyses, 3-axis interaction diagrams have been developed and compared with results for different wall friction angle. In addition, based on the numerical analyses, the nature of stresses developed in caisson because of soil resistance.

2 NUMERICAL MODELING

2.1 *Model properties*

3-dimensional model of square caisson embedded in layered soil strata was modeled using finite element-based software ABAQUS version 6.14 (SIMULIA 2014). The soil strata is composed of a 4.5m thick clay layer underlying a 3m sand layer and overlying a 4.5m thick sand layered followed by impermeable stratum.

The entire soil strata was modeled to be submerged. The extent of soil strata in the direction of loading is 30m and in the transverse direction is 20m. The square caisson with width (*B*) 1.5m and embedment depth (*D*) of 2.25m is subjected to a combination of vertical load (*V*), lateral load (*Q*) and moment (*M*).

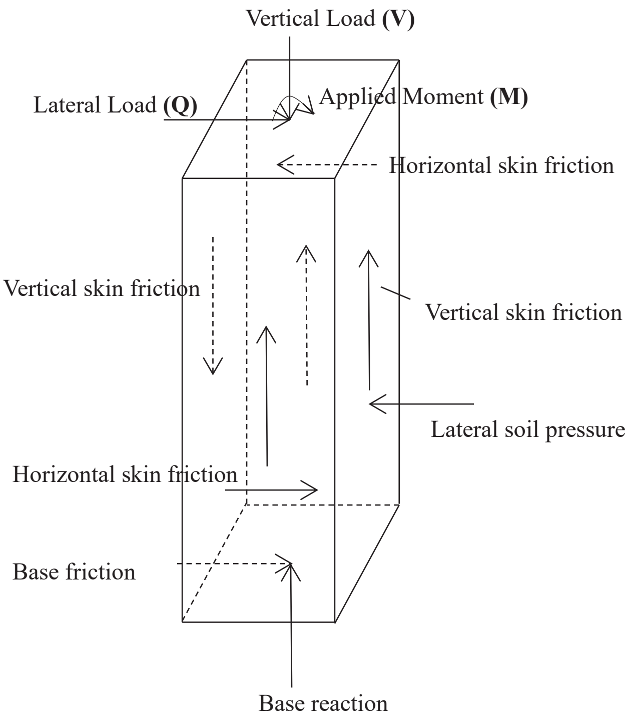

Figure 1. Soil reaction on different faces of caisson under applied loads

Sand has been modeled using elastic-Mohr-Coulomb plastic constitutive law. Clay elements were modeled using porous elastic - cam clay model constitutive model. 3-dimensional continuum brick elements with 8 nodes (C3D8R) were used to model caisson. 3-dimensional porous continuum brick elements with 8 nodes (C3D8RP) were used to model caisson. The reduced integration method of computation was carried out in order to save computational time without significantly compromising the accuracy of the model. In addition, Lagrangian multiplier method of constraint enforcement was used to model the interface between soil and caisson. The properties of sand and clay have been expressed in Table 1 and Table 2 respectively.

Fixed boundary was used to model the impermeable base of the strata whereas roller support has been used at side boundary. Geometric, material and contact non-linearity has been accounted for in the numerical analyses. The numerical model of caisson embedded in soil strata indicating the geometry, meshing, boundary condition and loading has been represented in Figure 2. The allowable vertical load has been obtained from stress-strain curve considering soil element just below the base of caisson and it was obtained as 1600 kN when considering a factor of safety of 3. The normalizing vertical load (V_n) for the current study has been calculated using correlation suggested by IS: 3955 (1967) given using Eqn. 1 as:

$$Q_a = 5.4N^2B + 16(100 + N^2)D \qquad (1)$$

where, Q_a is soil pressure in kg/m^2;
B is smaller section of caisson in m;
D is depth of caisson below scour level in m and
N is corrected Standard Penetration resistance.
V_n is then obtained as product of Q_a and base area.

The magnitude of normalizing vertical load is 1000kN for the given geometry and soil profile. The list of input properties adopted in the present study has been mentioned in Table 3.

Table 1. Properties of sand used in the numerical model

Property	Value
Elastic modulus (MPa)	90
Poisson's ratio [μ]	0.3
Unit weight [γ] (kN/m^3)	19
Coefficient of permeability (m/sec)	5×10^{-5}
Initial void ratio	0.8
Friction angle	30°
Dilation angle	1°

Table 2. Properties of clay used in the numerical model

Property	Value
Unit weight [γ] (kN/m^3)	17
Poisson's ratio [μ]	0.45
Slope of swelling line [κ]	0.075
Slope of virgin compression line [λ]	0.12
Coefficient of permeability (m/sec)	6×10^{-8}
Initial void ratio	0.9

Table 3. Properties of clay used in the numerical model

Parameter	Values
Base dimension (B)	1.5m ×1.5m
Embedment depth (D)	2.25m
Height of load application above scour level (H)	3.375m
Soil friction angle (ϕ)	30°
Wall friction angle (δ)	$\phi/2$
Horizontal seismic coefficient (k_h)	0, 0.1, 0.2 and 0.3
Vertical seismic coefficient (k_v)	0,0.5k_h and k_h
Normalized vertical load (V/V_n)	0.2, 0.4, 0.6, 0.8, 1, 1.2, 1.4 and 1.6
Lateral load for each V (Q/V)	0, 0.125, 0.25, 0.375, 0.5, 0.625, 0.75, 0.875 and 1

The vertical load is followed by application of 8 lateral loads of equal magnitudes. The entire loading process takes place in 45 steps wherein each vertical and lateral loading step is followed by 3 consolidation steps of increasing time intervals. During the consolidation steps, dissipation of excess pore pressure developed due to applied incremental loading takes place.

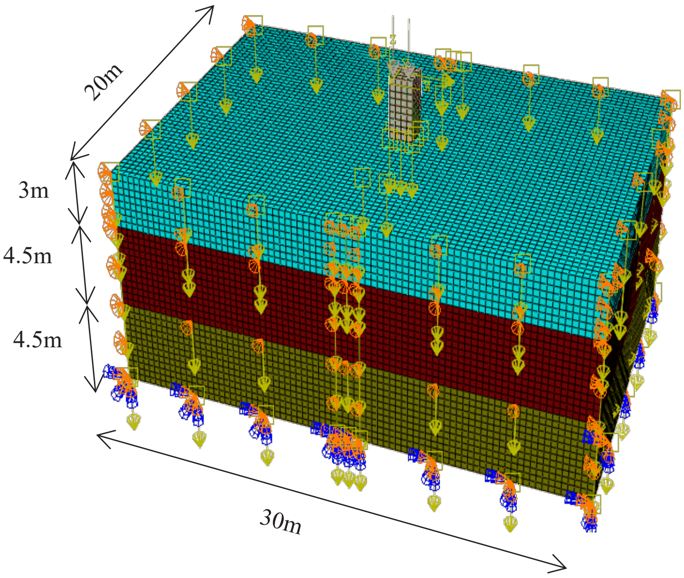

Figure 2. Numerical model of caisson embedded in soil strata indicating geometry, boundary conditions and loading

2.2 *Validation of model*

The actual field conditions were simulated in the current study with extensive details but in order to check the efficacy of the model, it was validated with the experimental work of Sharda (1975). The caisson geometry and soil profile adopted in the current study was same as that used in experimental study by Sharda (1975). In one of the tests, Sharda (1975) subjected the caisson with properties mentioned in Table 3 to vertical load of 1450 kg and then incremental lateral loads. The results were then presented in the form of plot between lateral soil pressure versus applied lateral load. The numerical model developed in the preceding section was subjected to identical vertical and lateral loads. The results of the analysis has been presented and compared with experimental results of Sharda (1975) in Figure 3. The magnitudes of lateral soil pressure from both the studies have been compared at a depth of 0.375 m. A maximum deviation of 6.98% from Sharda's (1975) result was observed which suggests that the field conditions have been simulated with excellent degree of accuracy.

3 RESULTS AND DISCUSSION

The numerical analyses for the set of input parameters mentioned in Table 3 were carried out and their results have been discussed in this section. All the calculations have been carried out using PYTHON programming language.

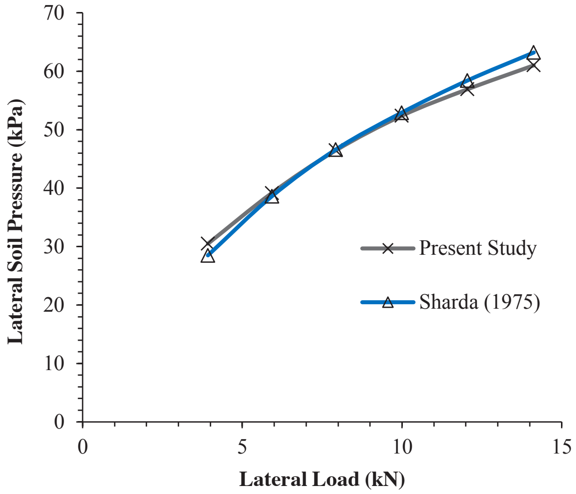

Figure 3. Validation of numerical model in present study with Sharda (1975)

3.1 *Lateral soil pressure*

Lateral soil pressure variation along depth of caisson has been shown in Figure 4 and Figure 5. From Figure 4, it can be seen that for V = 400kN and Q/V = 0.25, with increase of k_h from 0 to 0.1, 0.2 and 0.3, the percentage increase in lateral soil pressure value at a depth of 0.375m was 21.69%, 43.54% and 65.64% respectively. This increase may be attributed to the densification of soil causing increase in modulus of subgrade reaction and at the same time larger displacement of caisson due to increasing horizontal seismic inertia force. Because of the combined effect of these two factors, the increase in lateral soil pressure is observed. Similarly, the percentage increase for Q/V = 0.75 was 7.87%, 15.87% and 24.01% for increase in k_h from 0 to 0.1, 0.2 and 0.3 respectively.

When lateral load increases from 0.25 to 0.75, the percentage increase in lateral soil pressure was found to be 250.69%, 210.86%, 183.07% and 162.55% for k_h values of 0, 0.1, 0.2 and 0.3 respectively. Figure 5 compares the results of lateral soil pressure from present study with results for $\delta = \phi$. It was found that the percentage increase in lateral soil pressure for k_h values of 0, 0.1, 0.2 and 0.3 was 17.61%, 16.84%, 11.66% and 14.03% respectively when wall friction angle was decreased from $\delta = \phi$ to $\delta = \phi/2$. This is because of higher mobility offered to caisson because of reduction in soil-wall friction angle.

Along the width of caisson, lateral soil pressure is maximum at edges and minimum at the center of caisson at all depths because of higher stress concentration factor at edges. Factors like seismic acceleration coefficients, vertical and lateral load magnitude and wall friction angle have the same effect on lateral soil pressure along depth as they have on it along depth.

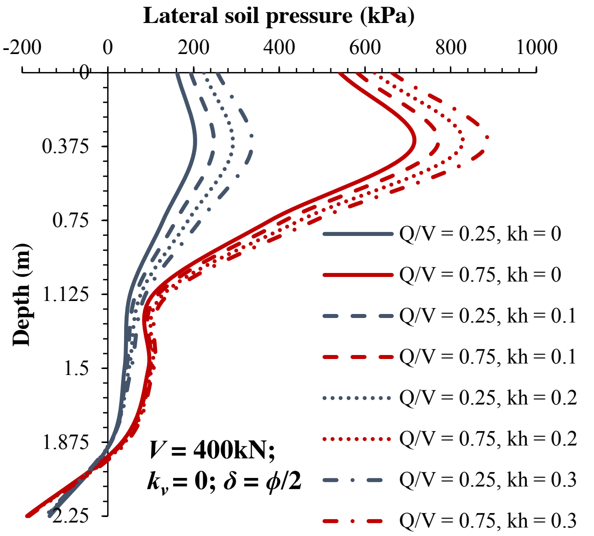

Figure 4. Variation of lateral soil pressure with depth for Q/V = 0.25 and Q/V = 0.75 for different k_h values

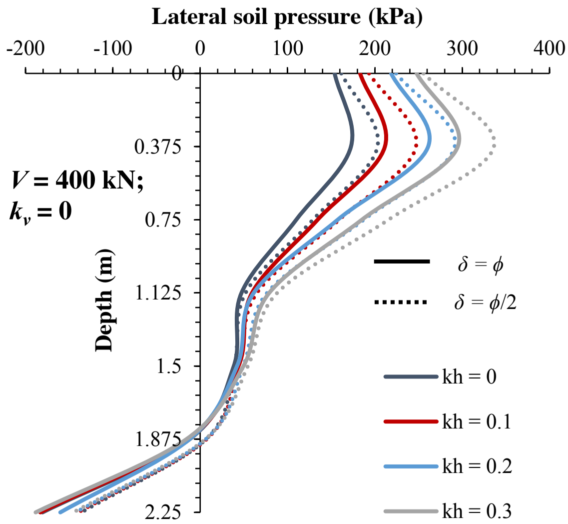

Figure 5. Variation of lateral soil pressure with depth for V = 400kN and Q/V = 0.25 for different δ and k_h values

3.2 *Tilt and shift of caisson*

Tilt and shift of caisson increase with increase in lateral load and horizontal and vertical seismic acceleration coefficient. However the tilt and shift magnitudes reduce with increase in soil-wall friction angle. The reasons for this behavior have been explained in previous section. Table 4 gives the magnitude of tilt of caisson in degrees for a vertical load of 400 kN, $\delta = \phi/2$ and different magnitudes of horizontal and vertical seismic acceleration coefficient. For V = 400 kN, Q/V = 0.75 and k_v/k_h = 0.5, as k_h increases from 0.1 to 0.2 and 0.3, tilt of caisson increases by 3.09% and 14.06% respectively. Similarly, for k_v = 0, as k_h is increased from 0 to 0.1, 0.2 and 0.3, the tilt of caisson increased by 4.6%, 5.22% and 15.29% respectively. Similar trend is observed for shift of caisson which has been depicted using Figure 6.

Table 4. Tilt of caisson for various input parameters

		Tilt of Caisson (°)							
k_h	k_v/k_h	Q/V = 0.125	Q/V=0.25	Q/V = 0.375	Q/V=0.5	Q/V= 0.625	Q/V = 0.75	Q/V = 0.875	Q/V = 1
0	0	0.24	0.62	1.04	1.51	2.04	2.62	3.28	4.01
0.1	0	0.28	0.69	1.11	1.60	2.15	2.74	3.44	4.14
	0.5	0.29	0.69	1.12	1.63	2.18	2.79	3.50	4.19
	1	0.20	0.65	1.13	1.70	2.33	3.04	3.83	4.57
0.2	0	0.22	0.63	1.06	1.58	2.14	2.76	3.47	4.15
	0.5	0.34	0.75	1.19	1.70	2.26	2.88	3.60	4.28
	1	0.26	0.76	1.33	2.00	2.74	3.59	4.41	5.55
0.3	0	0.40	0.82	1.27	1.80	2.36	3.02	3.76	4.42
	0.5	0.40	0.82	1.32	1.88	2.48	3.18	3.88	4.62

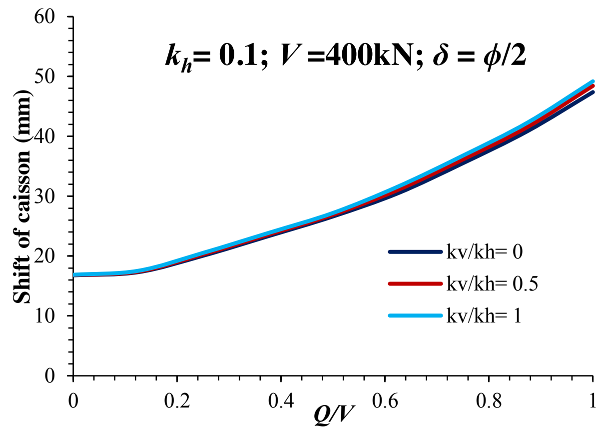

Figure 6. Variation of shift of caisson with lateral load for V = 400kN, k_h = 0.1 and $\delta = \phi/2$ for different and k_v values

3.3 *Depth of point of rotation*

Depth of point of rotation is one of the most direct measures of stability of caisson. The point of rotation of caisson moves upwards with increase in lateral loads and horizontal and vertical seismic acceleration coefficient and decrease in vertical load and soil-wall interface friction. As the point of rotation moves upwards, the depth of caisson experiencing passive resistance from soil against applied lateral load decreases which amounts to reduced stability of caisson. The variation of depth of point of rotation with horizontal seismic acceleration coefficient has been illustrated in Figure 7.

3.4 *Interaction Diagrams*

Interaction diagrams are graphical representation of combination of externally applied loads which cause failure in a system. In the present study, interaction diagrams relating applied vertical load (V), applied lateral load (Q) and applied moment (M) have been developed for $\delta = \phi/2$ and the results were compared with results for $\delta = \phi$. Failure is assumed to take place when tensile stress is developed in the soil below base of caisson as soil is weak in tension.

V has been normalized with respect to normalizing vertical load V_n which was determined in section 2.1 as 1000 kN. Q is normalized with respect to Q_n which is given as $Q_n = 0.45V_n$ (Kumar and Chatterjee, 2021). The normalizing moment M_n is defined as $M_n = Q_n \times (H+D)$.

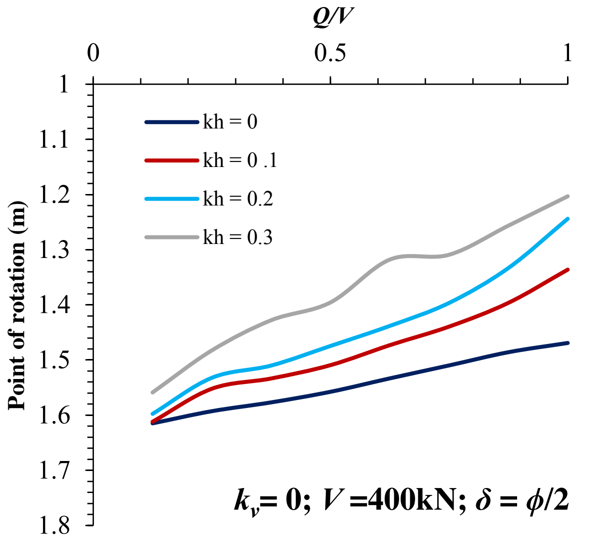

Figure 7. Variation of depth of point of rotation of caisson with lateral load for V = 400kN, k_v = 0 and $\delta = \phi/2$ for different and k_h values

The interaction diagrams were developed for different seismic cases and their behavior has been illustrated in Figure 8 and Figure 9.

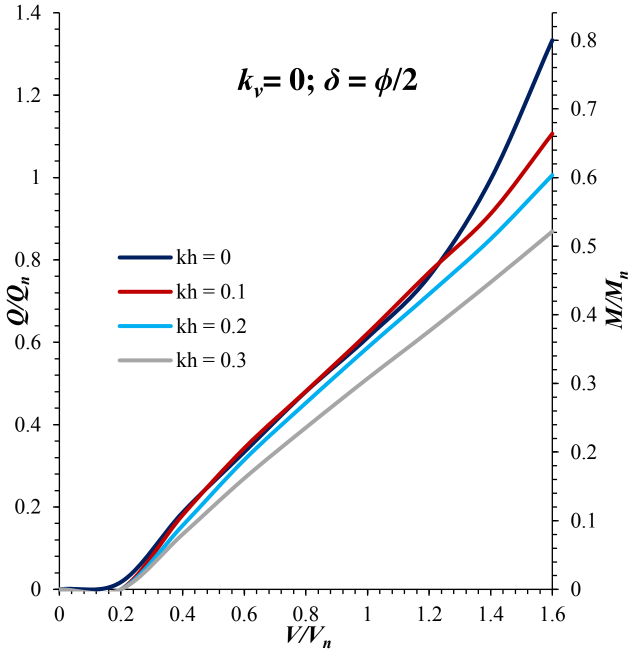

Figure 8. Normalized interaction diagram for k_v = 0 and $\delta = \phi/2$ for different and k_h values

Figure 8 reflects that as the magnitude of horizontal seismic acceleration coefficient increases, the capacity of caisson foundation system to withstand lateral load and moment for a given magnitude of vertical load decreases. At V/V_n = 1.4, when k_h increases from 0 to 0.1, 0.2 and 0.3 respectively, the capacity of caisson to carry lateral load and moment diminishes by 8.39%, 14.54% and 25.09% respectively.

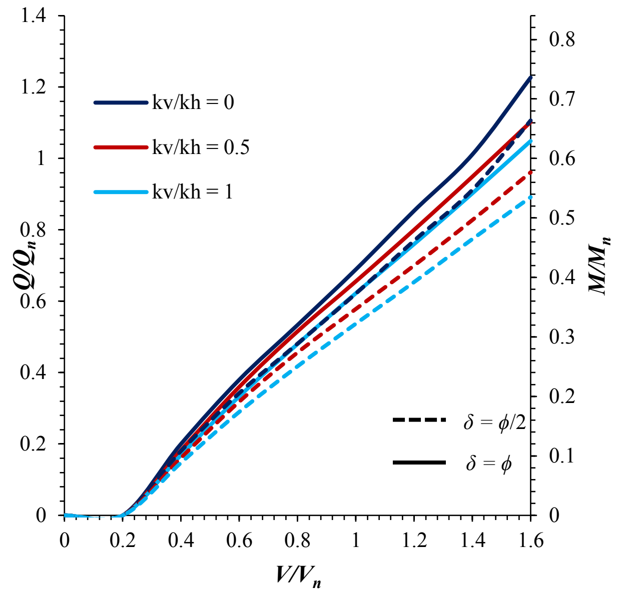

Figure 9. Normalized interaction diagram for k_h = 0.1, $\delta = \phi$ and $\delta = \phi/2$ for different k_v values

Figure 9 depicts the behavior of interaction diagrams with varying vertical seismic acceleration coefficient for k_h = 0.1. The results for $\delta = \phi$ is also presented in addition to $\delta = \phi/2$. The figure highlights that the load carrying capacity of caisson foundation system diminishes with increasing magnitude of k_v. However, load carrying capacity could be seen to improve with increase in magnitude of δ. The load carrying capacity for k_h = 0.1, k_v/k_h = 0.5 and V/V_n = 1.4 was 14.68% higher for $\delta = \phi$ compared to $\delta = \phi/2$.

4 CONCLUSIONS

The current study deals with the detailed modeling of caisson foundation system embedded in layered soil and also takes pore water pressure into account. The major conclusions drawn from this study are as follows:

- The nature of variation of lateral soil pressure, tilt and shift of caisson, depth of point of rotation with various input parameters have been studied and presented. It was observed that increase in seismic acceleration coefficients cause increase in lateral soil pressure whereas increase in soil-wall friction angle led to reduced lateral soil pressure.
- Tilt and shift of caisson also increased while point of rotation of caisson moved upwards with increase in seismic acceleration coefficient. These are clear indicators of instability in caissons.
- 3-axis interaction diagram in V-Q-M space was developed and compared with past results. It was seen that the capacity of caisson foundation system to carry lateral load and moment at a given vertical load decreases with increase in seismic acceleration coefficients.
- The load carrying capacity of a caisson foundation system increases with increasing soil-wall friction angle.

5 REFERENCES

Banerjee P. K. and Gangopadhyay S. 1960. Study on the stability of well foundations for major bridges. *Journal of Indian Roads Congress*. 22: 588–600.

Biswas S. and Choudhury D. 2019. Seismic soil resistance for caisson design in sand. *Proceeding of Institute of Civil Engineering.*

Geotechnical Engineering. 172 (1): 67–75. https://doi.org/10.1680/jgeen.17.00195.

Biswas S. and Choudhury D. 2020. Caissons in cohesionless soils considering 3D wedge under earthquake loading. *International Journal of Geomechanics*. 20 (12): 04020221_1-9.

BIS (Bureau of Indian Standard). 1967. Indian standard code of practice of design and construction of well foundation. IS: 3955. New Delhi: BIS.

Dominguez J. 1978. Dynamic stiffness of rectangular foundations. *Research Rep. No. R78-20*. Cambridge, MA: Dept. of Civil Engineering, Massachusetts Institute of Technology.

Gadre A. and Dobry R. 1998. Lateral cyclic loading centrifuge tests on square embedded footing. *Journal of Geotechnical and Geoenvironmental Engineering*. 124 (11): 1128–1138.

Gerolymos N. and Gazetas G. 2006. Winkler model for lateral response of rigid caisson foundations in linear soil. *Soil Dynamics and Earthquake Engineering*. 26 (5): 347–361.

Gerolymos N. Zafeirakos A. and Karapiperis K. 2015. Generalized failure envelope for caisson foundations in cohesive soil: Static and dynamic loading. *Soil Dynamics and Earthquake Engineering*. 78: 154–174.

Kumar M. and Chatterjee K. 2020. A numerical study on lateral load response of caissons in static conditions. *In Geo-Congress 2020: Foundations, Soil Improvement and Erosion*, Geotechnical Special Publication 315, edited by J. P. Hambleton, R. Makhnenko, and A. S. Budge, 15–22. Reston, VA: ASCE.

Kumar M. and Chatterjee K. 2021. Generalized interaction diagrams for caisson foundations in layered soil under seismic conditions. *International Journal of Geomechanics*.21(8): 04021135_1-14.

Mitta A. and Luco J. E. 1989. Dynamic response of a square foundation embedded in an elastic half-space. *Soil Dynamics and Earthquake Engineering*. 8 (2): 54–67.

Olson S.M. Hashash Y.M. Muszynski M.R. and Phillips C. 2017. Passive wedge formation and limiting lateral pressures on large foundations during lateral spreading. *Journal of Geotechnical and Geoenvironmental Engineering.* 143(7): 04017027_1-13.

Pender E. B. 1947. Lateral support afforded to piers founded in sand. *Journal of Institute of Engineering*. 19 (7): 151.

Sharda S. C. 1975. Response of well foundations under horizontal loads. *Ph.D. Thesis*, School of Research and Training in Earthquake Engineering, Univ. of Roorkee.

SIMULIA. 2014. *ABAQUS documentation* 6.14. Providence, RI: Dassault Systèmes.

Terzaghi, K. 1943. *Theoretical soil mechanics*. Hoboken, NJ: John Wiley & Sons.

Varun V. Assimaki D. and. Gazetas G. 2009. A simplified model for lateral response of large diameter caisson foundations—Linear elastic formulation. *Soil Dynamics and Earthquake Engineering*. 29 (2): 268–291.